

## Correlation of Mn charge state with the electrical resistivity of Mn doped indium tin oxide thin films

S. R. Sarath Kumar, Mohamed Nejb Hedhili, H. N. Alshareef, and S. Kasiviswanathan

Citation: *Applied Physics Letters* **97**, 111909 (2010); doi: 10.1063/1.3481800

View online: <http://dx.doi.org/10.1063/1.3481800>

View Table of Contents: <http://scitation.aip.org/content/aip/journal/apl/97/11?ver=pdfcov>

Published by the [AIP Publishing](#)

---

### Articles you may be interested in

[Ferromagnetism of manganese-doped indium tin oxide films deposited on polyethylene naphthalate substrates](#)

*J. Appl. Phys.* **105**, 07C511 (2009); 10.1063/1.3065965

[Ferromagnetism in sputtered manganese-doped indium tin oxide films with high conductivity and transparency](#)

*J. Appl. Phys.* **101**, 09H105 (2007); 10.1063/1.2710324

[Effects of SR irradiation on tin-doped indium oxide thin film prepared by rf magnetron sputtering](#)

*Rev. Sci. Instrum.* **73**, 1384 (2002); 10.1063/1.1423624

[Tin doped indium oxide thin films: Electrical properties](#)

*J. Appl. Phys.* **83**, 2631 (1998); 10.1063/1.367025

[Electronic transport in tin-doped indium oxide thin films prepared by sol-gel technique](#)

*J. Appl. Phys.* **83**, 2139 (1998); 10.1063/1.366949

---

An advertisement for Oxford Instruments Atomic Force Microscopy (AFM) systems. The background is a dark blue gradient. On the left, there is a mobile phone and a desktop computer. In the center, there is an AFM instrument. Text on the left side reads: "You don't still use this cell phone" and "or this computer". Text in the center reads: "Why are you still using an AFM designed in the 80's?". On the right side, text reads: "It is time to upgrade your AFM", "Minimum \$20,000 trade-in discount for purchases before August 31st", and "Asylum Research is today's technology leader in AFM". At the bottom right, there is the Oxford Instruments logo and the tagline "The Business of Science®". The email address "dropmyoldAFM@oxinst.com" is also present.

## Correlation of Mn charge state with the electrical resistivity of Mn doped indium tin oxide thin films

S. R. Sarath Kumar,<sup>1</sup> Mohamed Nejib Hedhili,<sup>1</sup> H. N. Alshareef,<sup>1,a)</sup> and S. Kasiviswanathan<sup>2</sup>

<sup>1</sup>King Abdullah University of Science and Technology, Thuwal 23955-6900, Saudi Arabia

<sup>2</sup>Department of Physics, Indian Institute of Technology Madras, Chennai 600036, India

(Received 17 May 2010; accepted 3 August 2010; published online 15 September 2010)

Correlation of charge state of Mn with the increase in resistivity with Mn concentration is demonstrated in Mn-doped indium tin oxide films. Bonding analysis shows that Mn  $2p_{3/2}$  core level can be deconvoluted into three components corresponding to  $Mn^{2+}$  and  $Mn^{4+}$  with binding energies 640.8 eV and 642.7 eV, respectively, and a  $Mn^{2+}$  satellite at  $\sim 5.4$  eV away from the  $Mn^{2+}$  peak. The presence of the satellite peak unambiguously proves that Mn exists in the +2 charge state. The ratio of concentration of  $Mn^{2+}$  to  $Mn^{4+}$  of  $\sim 4:1$  suggests that charge compensation occurs in the n-type films causing the resistivity increase. © 2010 American Institute of Physics. [doi:10.1063/1.3481800]

In the quest for a reliable spin polarized material for spintronic applications, intense research has been carried out on oxide thin films doped with transition metals.<sup>1,2</sup> Indium tin oxide (ITO) thin films, which are n-type transparent conducting oxides with a band gap of  $\sim 3.75$  eV,<sup>3</sup> when doped with transition metals in few atomic percentages can become diluted magnetic semiconductors (DMS), thus forming an important class of materials for diverse technological applications.<sup>1</sup> A DMS is formed by doping a nonmagnetic semiconductor, usually, with a few atomic percent of one or more transition metals and the spins of the transition metal ions retain their remanent alignment under the influence of spin polarized carriers.<sup>4</sup> The excellent electrical conductivity and reasonable mobility combined with the high optical transparency which makes ITO one of the most widely used transparent electrodes in liquid crystal displays, solar cells, and electrochromic devices,<sup>3</sup> also make it an excellent host matrix for developing a DMS. Thin films of ITO doped with transition metals such as Fe, Co, Ni, Cr, and Mn have been found to exhibit room temperature ferromagnetism,<sup>5,6</sup> which is one of the prerequisites for these films to be used in spintronic devices.<sup>4</sup>

The key to optimizing the properties of the transition metal doped ITO films is an understanding of the chemical environment of the dopant in the semiconductor matrix. It has been observed that the charge state of the transition metal dopant strongly influences the electrical and magnetic properties of DMS films.<sup>6,7</sup> For instance, increase in Mn concentration has been found to result in an increase in resistivity and a decrease in magnetization in Mn doped  $SnO_2$ .<sup>8</sup> It has been reported that when doped with Mn, ZnO becomes highly conductive at high temperatures but resistive at room temperature, depending on the Mn concentration.<sup>9</sup> In Mn doped CuO films, the observed increase in resistivity with Mn doping has been assumed to be due to the  $Mn^{2+}$  ions, even though x-ray photoelectron spectroscopy (XPS) results were inconclusive of the presence of  $Mn^{3+}$  and  $Mn^{4+}$  ions.<sup>10</sup> The presence of  $Mn^{2+}$  ions has also been invoked to explain the sharp decrease in lattice constant of Mn doped ITO

(Mn:ITO) film as compared to that of undoped ITO film.<sup>7</sup> In light of these reports, the possible existence of multiple charge states of Mn which make any predictions on the properties of the grown films difficult has to be expected in Mn:ITO films. Hence, it is important that oxidation state of Mn in the films be identified. Here, we report XPS studies on the charge state of Mn and its influence on the electrical resistivity of Mn:ITO films.

Several methods such as reactive thermal evaporation,<sup>7</sup> pulsed laser deposition,<sup>5,11</sup> rf magnetron sputtering,<sup>12</sup> and sol-gel<sup>13</sup> have been used to grow Mn:ITO thin films. In the present work the films were deposited using dc reactive sputtering on Si and Si/SiO<sub>2</sub> substrates, as described elsewhere.<sup>14</sup> The Mn compositions of the films reported here were obtained using Rutherford backscattering spectroscopy.<sup>15</sup> Mn:ITO films sputtered with two different targets was estimated to have 1.6 and 4.3 at. % Mn. These films will be henceforth referred to as 1.6% Mn:ITO and 4.3% Mn:ITO, respectively. Similar Mn:ITO films on Si/SiO<sub>2</sub> substrates had exhibited room temperature ferromagnetism.<sup>15</sup> Grazing incidence x-ray diffraction (GIXRD) was used to identify the phase as well as lattice constants of the films. XPS was extensively used to identify the oxidation state of Mn in the films. Electrical resistivity measurements of the films grown on Si/SiO<sub>2</sub> substrates were performed as a function of temperature, using the linear four-probe method to bring out the effect of Mn doping.

Figure 1(a) shows the GIXRD pattern obtained for 4.3% Mn:ITO films on Si substrate. The patterns could be indexed based on the cubic bixbyite structure of ITO. The films were polycrystalline with mean crystallite sizes in the range 40–80 nm. When compared to ITO films, no additional peaks corresponding to any secondary phases could be detected in Mn:ITO films. However, there is a systematic shift in the (222) peak position toward lower “d” values with increasing Mn concentration as shown in Fig. 1(b). The calculated lattice constant ( $10.10 \pm 0.01$  Å) of ITO film matches well with the reported value.<sup>7</sup> The lattice constants of 1.6% Mn:ITO and 4.3% Mn:ITO films have been calculated as  $10.06 \pm 0.01$  Å and  $10.03 \pm 0.01$  Å, respectively. A similar effect wherein a decrease in lattice constant with increase in Mn content had been observed in films deposited on glass

<sup>a)</sup>Author to whom correspondence should be addressed. Electronic mail: husam.alshareef@kaust.edu.sa.

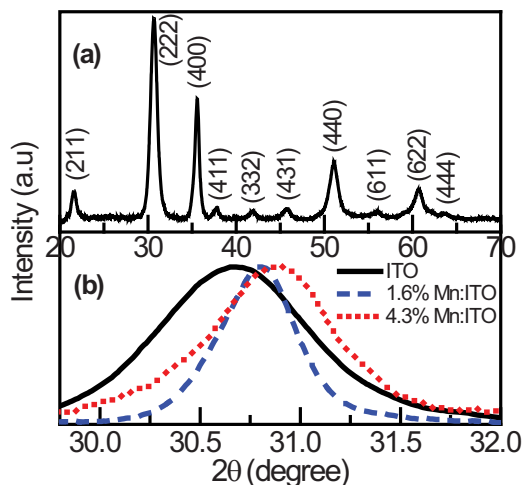


FIG. 1. (Color online) (a) GXR pattern of 4.3% Mn:ITO film and (b) shift in (222) peak position of ITO thin film with Mn doping.

substrates as well.<sup>15</sup> To explain the decrease in lattice constant, it has often been suggested that  $\text{Sn}^{4+}$  and  $\text{Mn}^{2+}$  ions having smaller ionic radii (0.83 Å and 0.81 Å, respectively) substitute for larger (0.94 Å)  $\text{In}^{3+}$  ions in an octahedral configuration in Mn:ITO films.<sup>7</sup> It is to be noted here that  $\text{Mn}^{3+}$  and  $\text{Mn}^{4+}$  ions also have smaller ionic radii (0.72 and 0.67 Å) and it is possible that these ions may also be present. However, in the previous reports<sup>7,12,13</sup> there was little evidence of the charge state of Mn making an unambiguous explanation difficult. Hence, a detailed XPS study has been performed on the films to bring out the charge state of Mn.

XPS studies were carried out in a Kratos Axis Ultra DLD spectrometer equipped with a monochromatic Al K $\alpha$  x-ray source ( $h\nu=1486.6$  eV) operating at 150 W, a multi-channel plate and delay line detector under a vacuum of  $\sim 10^{-9}$  mbar. Measurements were performed in hybrid mode using electrostatic and magnetic lenses, and the take-off angle (angle between the sample surface normal and the electron optical axis of the spectrometer) was  $0^\circ$ . All spectra were recorded using an aperture slot of  $300 \mu\text{m} \times 700 \mu\text{m}$ . The survey and high-resolution spectra were collected at fixed analyzer pass energies of 160 eV and 20 eV, respectively. Samples were mounted in floating mode in order to avoid differential charging.<sup>16</sup> Charge neutralization was required for all samples. Binding energies were referenced to the C 1s binding energy of adventitious carbon contamina-

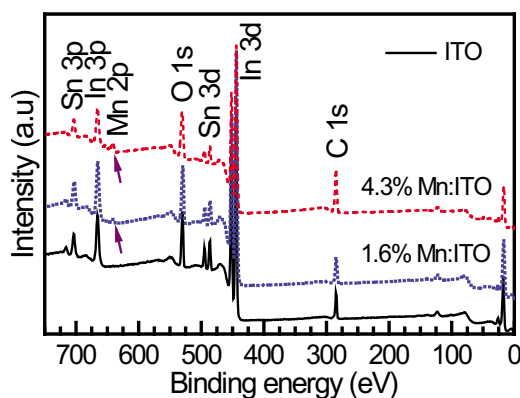


FIG. 2. (Color online) (a) XPS Survey spectra of ITO (solid line), 1.6% Mn:ITO (dotted line), and 4.3% Mn:ITO (dashed line). The increase in Mn 2p peak intensity (indicated by the arrows) with Mn concentration of the doped films is clearly seen.

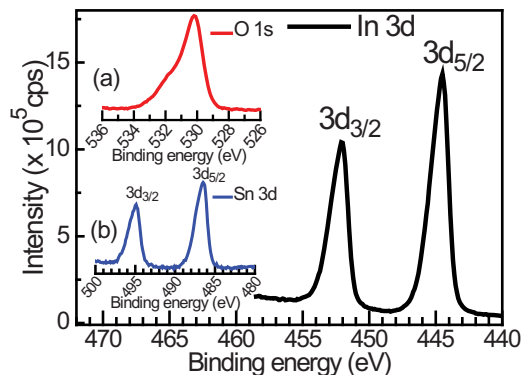


FIG. 3. (Color online) High resolution XPS spectra of In 3d core level. Insets (a) and (b) show the high resolution XPS spectra of O 1s and Sn 3d core levels, respectively.

tion which was taken to be 285.0 eV. The data were analyzed with commercially available software, CASAXPS. The individual peaks were fitted by a Gaussian (70%)–Lorentzian (30%) (GL30) function after Shirley type background subtraction.

The XPS survey spectra obtained from ITO, 1.6% Mn:ITO and 4.3% Mn:ITO films are shown in Fig. 2. Four major peaks corresponding to In (In 3d), Sn (Sn 3d), O (O 1s), and C (C 1s) for ITO film and an additional (Mn 2p) peak for the Mn:ITO films can be clearly seen. The presence of C 1s peak in the spectra is due to atmospheric contaminants, which could be removed by  $\text{Ar}^+$  sputtering of the films. It is observed that the intensity of Mn (Mn 2p) peak increases with the Mn concentration. High resolution XPS spectra of In 3d, Sn 3d, and O 1s core levels have also been obtained and are shown in Fig. 3. For ITO film, the observed binding energies of 444.5, 486.5, and 530.2 for In 3d<sub>5/2</sub>, Sn 3d<sub>5/2</sub> and O 1s core levels, respectively, are in excellent agreement with the values reported in previous studies,<sup>17–19</sup> where ITO films were grown using different techniques. The binding energies of In 3d<sub>5/2</sub> and Sn 3d<sub>5/2</sub> indicates the charge state of In and Sn is predominantly +3 and +4, respectively, which is expected for good quality ITO films.<sup>17–19</sup>

Figure 4 shows high-resolution XPS spectrum of Mn 2p<sub>3/2</sub> core level from 4.3% Mn:ITO film along with the deconvoluted components. The Mn 2p<sub>3/2</sub> line centered at  $\sim 641.2$  eV was fitted using three components. The first

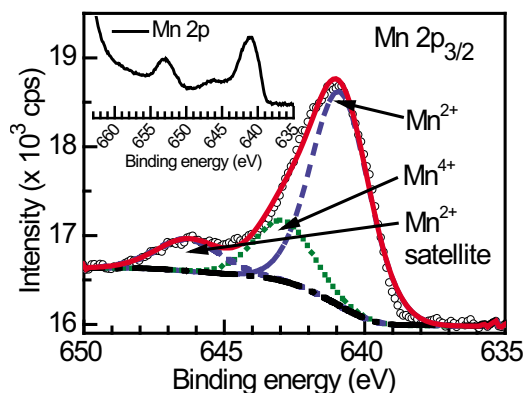


FIG. 4. (Color online) Mn 2p<sub>3/2</sub> core level XPS experimental spectra (open circles) along with the deconvoluted components: Mn<sup>2+</sup> peak and satellite (dashed lines), Mn<sup>4+</sup> peak (dotted line) and the overall fit (solid line). The inset shows the Mn 2p core level spectra (including the Mn 2p<sub>1/2</sub> core level).

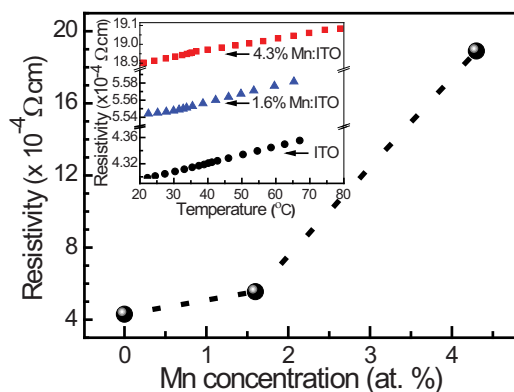


FIG. 5. (Color online) Variation in resistivity at 25 °C with Mn concentration for Mn:ITO films. The dotted line is only to guide the eye. The variation in resistivity of ITO (circles), 1.6% Mn:ITO (triangles), and 4.3% Mn:ITO films (squares) with temperature is shown as inset.

component is centered at  $\sim 640.8$  eV. Its position is in agreement with the binding energy of  $\text{Mn}^{2+}$  as in  $\text{MnO}$ .<sup>20–23</sup> The second component centered at  $\sim 642.7$  eV is attributed to  $\text{Mn}^{4+}$  as in  $\text{MnO}_2$ .<sup>23,24</sup> It is to be mentioned here that metallic Mn has a  $2p_{3/2}$  line at 639 eV, while the line from  $\text{Mn}^{3+}$  has a binding energy of  $\sim 641.7$  eV.<sup>21,23,25</sup> The observation of a satellite line (third component) spaced by  $\sim 5.4$  eV from the first component further supports that the dominant contribution is from  $\text{Mn}^{2+}$ . The satellite excitation is typical for  $\text{MnO}$  (Refs. 26 and 27) and is not present in either  $\text{Mn}_2\text{O}_3$  or  $\text{MnO}_2$  (Refs. 28–31) and is considered as a signature of the presence of  $\text{Mn}^{2+}$  as in  $\text{MnO}$ . A similar satellite peak for Mn  $2p_{1/2}$  is however buried in the tail region of In  $3p_{3/2}$  for Mn:ITO films, as shown as inset to Fig. 4 and hence is barely observed. From the integrated area under each component, the ratio of  $\text{Mn}^{2+}$  to  $\text{Mn}^{4+}$  is evaluated to be  $\sim 4:1$ , indicating that the dominant valance state of Mn in Mn:ITO films is +2. Deconvolution using different backgrounds (Tougaard and an exponential-like background with Shirley component) to account for the contribution of the tail of In  $3p_{3/2}$  peak yielded similar results. Furthermore, the  $\sim 4:1$  ratio is also obtained for the 1.6% Mn:ITO film.

The room temperature resistivity of the films as a function of Mn concentration is shown in Fig. 5. The observed increase in the resistivity of the films (from 0.43 to 1.89 m $\Omega$  cm) with increasing Mn concentration is explained using the results from XPS analysis. The charge state of the Mn ions that substitute for  $\text{In}^{3+}$  and/or  $\text{Sn}^{4+}$  ions has a direct impact on the electrical properties of the films. In fact, incorporation of  $\text{Mn}^{2+}$  ions reduces the carrier concentration<sup>7</sup> while  $\text{Mn}^{4+}$  ions, like  $\text{Sn}^{4+}$  ions, can contribute additional electrons to the conduction band. However, since Mn ions enter the lattice predominantly as  $\text{Mn}^{2+}$ , Mn incorporation effectively results in hole doping which amounts to charge compensation of the n-type films. The decrease in the carrier concentration of the films directly results in the increase in resistivity with increasing Mn concentration. Though predominant doping by  $\text{Mn}^{2+}$  ions having higher magnetic moments compared to that of  $\text{Mn}^{4+}$  ions is desirable for improving the magnetic properties of the films, it essentially results in increasing the resistivity. The variation in resistivity of the films with temperature shown as inset to Fig. 5 reveals the metal-like behavior of ITO and the Mn:ITO films. It is to be noted here that ITO, depending upon the growth conditions, can exhibit a semiconductor to metal transition at around

room temperature.<sup>32</sup> The observed metal-like behavior may be attributed to enhanced scattering of the carriers, with increase in temperature, which negates the contribution to conductivity by the thermally activated carriers.<sup>32</sup> Since Mn doping only increases the resistivity without altering the metal-like behavior, alternative growth conditions such as lower oxygen partial pressure during sputtering and additional  $\text{Sn}^{4+}$  doping may help improve the electrical properties without significantly affecting the magnetic properties of the films.

In summary, dc reactive sputtered Mn:ITO films with varying Mn concentration have been grown. The dominant charge state of Mn in the films is found to be +2 and is directly correlated with the observed increase in resistivity with increase in Mn concentration. The results imply that additional strategies need to be employed to independently tune the magnetic and electrical properties effectively in Mn:ITO films.

- <sup>1</sup>S. A. Chambers, T. C. Droubay, C. M. Wang, K. M. Rosso, S. M. Heald, D. A. Schwartz, K. R. Kittilstved, and D. R. Gamelin, *Mater. Today* **9**, 28 (2006).
- <sup>2</sup>T. Dietl and H. Ohno, *Mater. Today* **9**, 18 (2006).
- <sup>3</sup>T. Minami, *Semicond. Sci. Technol.* **20**, S35 (2005).
- <sup>4</sup>S. A. Chambers, *Surf. Sci. Rep.* **61**, 345 (2006).
- <sup>5</sup>M. Venkatesan, R. D. Gunning, P. Stamenov, and J. M. D. Coey, *J. Appl. Phys.* **103**, 07D135 (2008).
- <sup>6</sup>J. Stankiewicz, F. Villuendas, J. Bartalomé, and J. Sezé, *J. Magn. Magn. Mater.* **310**, 2084 (2007).
- <sup>7</sup>J. Philip, N. Theodoropoulou, G. Berera, J. S. Moodera, and B. Satpati, *Appl. Phys. Lett.* **85**, 777 (2004).
- <sup>8</sup>H. Kimura, T. Fukumura, M. Kawasaki, K. Inaba, T. Hasegawa, and H. Koinuma, *Appl. Phys. Lett.* **80**, 94 (2002).
- <sup>9</sup>J. Han, P. Q. Mantas, and A. M. R. Senos, *J. Eur. Ceram. Soc.* **22**, 49 (2002).
- <sup>10</sup>H. Zhu, F. Zhao, L. Pan, Y. Zhang, C. Fan, Y. Zhang and J. Q. Xiao, *J. Appl. Phys.* **101**, 09H111 (2007).
- <sup>11</sup>T. Ohno, T. Kawahara, H. Tanaka, T. Kawai, M. Oku, K. Okada, and S. Kohiki, *Jpn. J. Appl. Phys., Part 2* **45**, L957 (2006).
- <sup>12</sup>T. Nakamura, K. Tanabe, K. Tsureishi and K. Tachibana, *J. Appl. Phys.* **101**, 09H105 (2007).
- <sup>13</sup>S. Kundu, D. Bhattacharya, J. Ghosh, P. Das, and P. K. Biswas, *Chem. Phys. Lett.* **469**, 313 (2009).
- <sup>14</sup>S. R. Sarath Kumar and S. Kasiviswanathan, *Semicond. Sci. Technol.* **24**, 025028 (2009).
- <sup>15</sup>S. R. Sarath Kumar, P. Malar, T. Osipowicz, S. S. Banerjee, and S. Kasiviswanathan, *Nucl. Instrum. Methods Phys. Res. B* **266**, 1421 (2008).
- <sup>16</sup>Y. Mori, M. Tanemura, and S. Tanemura, *Appl. Surf. Sci.* **228**, 292 (2004).
- <sup>17</sup>A. J. Nelson and A. Aharoni, *J. Vac. Sci. Technol. A* **5**, 231 (1987).
- <sup>18</sup>W. Wu, B. Chiou, and S. Hsieh, *Semicond. Sci. Technol.* **9**, 1242 (1994).
- <sup>19</sup>H. S. Majumdar, S. Majumdar, D. Tobjörk, and R. Österbacka, *Synth. Met.* **160**, 303 (2010).
- <sup>20</sup>M. A. Langell, C. W. Hutchings, G. A. Carson, and M. H. Nassir, *J. Vac. Sci. Technol. A* **14**, 1656 (1996).
- <sup>21</sup>C. N. R. Rao, D. D. Sarma, S. Vasudevan, and M. S. Hedge, *Proc. R. Soc. London, Ser. A* **367**, 239 (1979).
- <sup>22</sup>J. S. Foord, R. B. Jackman, and G. C. Allen, *Philos. Mag. A* **49**, 657 (1984).
- <sup>23</sup>R. J. Iwanowski, M. H. Heinonen, and E. Janik, *Chem. Phys. Lett.* **387**, 110 (2004).
- <sup>24</sup>Y. Umezawa and C. N. Reilley, *Anal. Chem.* **50**, 1290 (1978).
- <sup>25</sup>M. Oku and K. Hirokawa, *J. Electron Spectrosc. Relat. Phenom.* **8**, 475 (1976).
- <sup>26</sup>F. Müller, R. de Masi, D. Reinicke, P. Hufner, and K. Stowe, *Surf. Sci.* **520**, 158 (2002).
- <sup>27</sup>S. P. Jeng, R. J. Lad, and V. E. Henrich, *Phys. Rev. B* **43**, 11971 (1991).
- <sup>28</sup>S. A. Chambers and Y. Liang, *Surf. Sci.* **420**, 123 (1999).
- <sup>29</sup>M. A. Stranick, *Surf. Sci. Spectra* **6**, 31 (1999).
- <sup>30</sup>M. A. Stranick, *Surf. Sci. Spectra* **6**, 39 (1999).
- <sup>31</sup>M. C. Militello and S. W. Gaarenstroom, *Surf. Sci. Spectra* **8**, 200 (2001).
- <sup>32</sup>Y. Li, C. Li, D. He, and J. Li, *J. Phys. D: Appl. Phys.* **42**, 105303 (2009).